Dynamics of the angular momentum in narrow quantum rings with Rashba and Dresselhaus spin-orbit interactions

J. M. Lia,[1] P. I. Tamborenea,[1] M. Cygorek,[2] and V. M. Axt[3]

[1]*Departamento de Física and IFIBA, FCEN, Universidad de Buenos Aires, Ciudad Universitaria, Pab. I, C1428EHA Buenos Aires, Argentina*

[2]*SUPA, Institute of Photonics and Quantum Sciences, Heriot-Watt University, Edinburgh EH14 4AS, United Kingdom*

[3]*Theoretische Physik III, Universität Bayreuth, 95440 Bayreuth, Germany*

(Received 17 September 2021; revised 28 February 2022; accepted 11 March 2022; published 24 March 2022)

The quantum dynamics of the electron's spin and orbital angular momenta in semiconductor quantum rings is analyzed. Both Rashba and Dresselhaus spin-orbit interactions (SOIs) in their quasi-two-dimensional forms are taken into account. The narrow quantum rings are treated with models including one and two radial modes. We find that when either Rashba or Dresselhaus SOI acts alone, the different angular momentum states are coupled in blocks of two (for a single radial mode) or four (for two radial modes). We also show that the full Hilbert space splits into two disjoint subspaces, which are not coupled by either of the two SOIs, thereby decoupling accordingly the state evolution. When both SOI mechanisms are present, in principle infinitely many states are coupled, but we find by numerical computation of the quantum dynamics that for typical evolution times in practice only a few neighboring states are involved in the dynamics. Thus the exchange of angular momenta proceeds only via very few states. Furthermore, we find a trend that when initially high orbital momenta are prepared, the time evolution of spin and orbital momenta is almost unaffected by the availability of a second radial mode, in sharp contrast to the case of preparing the system in low orbital angular momentum states. The implications of our findings for the coherent control of angular momentum in quantum rings are pointed out.

DOI: 10.1103/PhysRevB.105.115426

I. INTRODUCTION

The spin-orbit interaction (SOI) in quasi-two-dimensional (quasi-2D) semiconductor systems has important consequences in their electronic properties [1,2]. Many spin-based devices rely on the spin-orbit interaction [3], since it allows the control of the spin degree of freedom via applied voltages (electric fields). On the other hand, sometimes this interaction can hinder applications by causing dephasing and decoherence, just by itself or in combination with the electron-phonon interaction [4]. Another, physically obvious, effect of any SOI is to generally produce an interchange between orbital and spin angular momenta (OAM and SAM, respectively) during the quantum evolution. This effect is rather small in the classic case of the $n = 2$ shell of the hydrogen atom, but it can be much more relevant for a single electron in the presence of the Rashba interaction in semiconductor structures. Indeed, the Rashba interaction, which appears when the structural inversion symmetry is broken [1,5], cannot be considered a small perturbation as it modifies the electron energy levels noticeably. Despite this encouraging fact—from the point of view of controlling the angular momenta—it has been shown that in an extended quasi-2D electron gas the effective SOIs do not induce a significant interchange between spin and orbital angular momentum. This insensitivity of the spin dynamics to the orbital angular momentum of the carriers in extended systems, observed experimentally in Ref. [6] and explained theoretically in Ref. [7], is due to the fact that, with increasing system size, the set of total angular momentum eigenstates within a narrow energy window resembles more and more a translationally invariant manifold with respect to the total angular momentum quantum number j. The concrete value of j therefore plays no significant role in the subsequent spin dynamics in extended systems. Yet, this can be overcome in mesoscopic structures where finite confinement energies break this translational invariance.

The most natural candidates to explore the dynamics and control of angular momentum are then rotationally invariant quantum dots [8,9] and rings (QRs) [10]. Quantum rings formed inside quasi-2D structures display Rashba and Dresselhaus interactions like those of their host quantum wells. (We mention that the Dresselhaus SOI was first introduced to describe the spin-split conduction band of semiconductors lacking bulk inversion symmetry [11], but it also manifests itself in semiconductor systems of reduced dimensionality [1].) These systems have been modeled by Meijer *et al.* [12] and by Shakouri *et al.* [13] considering one and two lateral (radial) wave functions, respectively. The effects of the Rashba and Dresselhaus SOIs on QRs have attracted a great deal of attention in the last two decades [14–26]. A solution to the energy eigenvalue problem within the model of Meijer *et al.* including Rashba and Dresselhaus interactions simultaneously has been found [27,28]. Here we study QRs with SOI within the two cited models from the point of view of quantum dynamics, in order to clarify and systematize the role of the SOIs acting individually and simultaneously. We find that the SOIs produce nonperturbative effects in the interplay between OAM and SAM for realistic material parameters,

which would enable meaningful quantum control operations. At the same time we show that intrinsic limitations appear in the dynamics due to the decoupling of the Hilbert space into two- and four-level systems when only one SOI is present and a single or two radial modes are accounted for, respectively. Also, we show that the full Hilbert space is divided into two disjoint subspaces not coupled by either SOI—a fact that deeply affects the evolution of the angular momenta.

The work presented here attempts to contribute ultimately to the important technological goal of optical control of the magnetization [29–31]. Specifically, we have in mind a scheme where OAM is transferred to the electrons in the solid from optical vortices [32], and subsequently this OAM is converted to SAM via the spin-orbit interaction. The latter step is the one that we are elucidating here from a dynamical point of view for a single electron in QR. In this way one would manipulate the SAM of the charge carriers, which is responsible for the interaction with the magnetic impurities in dilute magnetic semiconductors [33,34], thereby controlling indirectly the magnetization.

The paper is organized as follows. In Sec. II we present the QR system, its Hamiltonian in the model of Meijer *et al.*, and explain the decouplings of the Hilbert space. In Sec. III A we study the quantum dynamics with only one SOI and in Sec. III B we consider the case with both Rashba and Dresselhaus SOIs acting simultaneously. In Sec. IV we extend the previous results to the model of Shakouri *et al.* and compare both models. Section V provides a summary of the main results and concluding remarks.

II. QUANTUM RING SYSTEM

We write the single-particle Hamiltonian in the envelope-function approximation as

$$H = -\frac{\hbar^2}{2m^*}\nabla^2 + V(\mathbf{r}) + H_R + H_D, \tag{1}$$

where m^* is the conduction-band effective mass and $V(\mathbf{r})$ the external confining potential of the ring. In what follows, we will group these two terms under the name H_0, that is, we set $H_0 = -\hbar^2\nabla^2/(2m^*) + V(\mathbf{r})$. The system is considered to be quasi-two-dimensional and the z dependence is henceforth integrated out as usual. The Rashba and Dresselhaus interactions are taken into account separately through H_R and H_D, respectively, which are linear in the momentum and read

$$H_R = i\alpha(k_-\sigma_+ - k_+\sigma_-) \quad \text{and} \quad H_D = \beta(k_+\sigma_+ + k_-\sigma_-). \tag{2}$$

In these definitions α and β are the coupling constants, $\sigma_\pm = (\sigma_x \pm i\sigma_y)/2$, where σ_x and σ_y are Pauli matrices, and $k_\pm = k_x \pm ik_y$, where $k_{x,y} = -i\partial_{x,y}$ are the in-plane components of the momentum. It can be shown directly from the form of H_R and H_D that the former conserves J_z, while the latter conserves $L_z - S_z$; that is, $[H_R, J_z] = [H_D, L_z - S_z] = 0$ (see Appendix A).

Here we will work with two effective Hamiltonians that, although derived from quite different approximations to H, both respect the axial symmetry of the QR in the absence of SOI. In other words, we will only consider approximations to H_0 that satisfy the condition $[H_0, L_z] = 0$. Since H_0 is independent of spin, it also holds that $[H_0, J_z] = 0$. Therefore, an arbitrary rotation generated by the total angular momentum operator around the axis of the ring leaves the effective H_0 invariant. The inclusion of SOI does not break this symmetry completely, but sharply reduces it to only rotations by π around the same axis. This means that even when SOI is present the effective full Hamiltonian satisfies $RHR^{-1} = H$, with $R = e^{-iJ_z\pi/\hbar}$. This persisting symmetry splits the Hilbert space into at least two disjoint subspaces, which correspond to independent blocks in the matrix representation of H. To see this, take the basis for the Hilbert space to be the set of all J_z eigenstates with eigenvalues j_z and notice that the action of R on any of them only shifts its global phase by either $\pm i$, depending on whether $j_z + 1/2$ is even or odd. Then, it is not hard to show that $\langle j_z|H|j_z'\rangle = 0$ if this global phase shift is different for $|j_z\rangle$ and $|j_z'\rangle$. In more formal terms, the electron wave functions with definite j_z transform according to two different irreducible representations (Γ_3 and Γ_4) of the (cyclic) double group C_2 (see Refs. [35,36]). The representation to which each wave function belongs is given precisely by the global phase it gains under the action of R, which coincides with the character of this operation in that representation.

III. NARROW-RING APPROXIMATION

Let us now consider the method developed by Meijer *et al.* [12]. This method allows us to obtain an effective Hamiltonian for a very narrow, quasi-one-dimensional ring. For convenience, in what follows we will express all operators in polar coordinates (r, φ). In this method the eigenstates of the purely transversal terms in H_0 are separated from the remaining terms in H and factorized into products of radial and azimuthal modes. For very narrow QRs, the energy scale of the latter is smaller than that of the former to such an extent that it is reasonable to assume that electrons occupy only the lowest radial mode, lacking the energy to make transitions to modes of higher energy. An effective one-dimensional azimuthal Hamiltonian is then obtained by taking the expectation value of the remaining terms in H over this common radial mode. Following this procedure, the operators $k_\pm$ in H_R and H_D become $k_\pm = ia^{-1}e^{\pm i\varphi}(\pm\hbar^{-1}L_z + 1/2)$, and the first two terms of H reduce to $H_0 = E_0L_z^2/\hbar^2$, with $E_0 = \hbar^2/2m^*a^2$. Moreover, it can be argued that the form of these operators does not depend on the particular confinement in the radial direction [12], which is assumed to have cylindrical symmetry.

To analyze the dynamics induced by this effective Hamiltonian we will consider the space spanned by the set of J_z eigenstates $\{|\ell, \sigma\rangle : \ell \in \mathbb{Z}, \sigma = \pm 1/2\}$, which are also eigenstates of H_0. The individual action of H_R and H_D on any state $|\ell, \sigma\rangle$ is straightforward:

$$H_R|\ell, \sigma\rangle = \hbar\omega_R(\ell + \sigma)|\ell + 2\sigma, \bar{\sigma}\rangle, \tag{3}$$

$$H_D|\ell, \sigma\rangle = 2\sigma i\hbar\omega_D(\sigma - \ell)|\ell - 2\sigma, \bar{\sigma}\rangle, \tag{4}$$

where $\bar{\sigma} = -\sigma$, $\hbar\omega_R = \alpha/a$, and $\hbar\omega_D = \beta/a$. The conservation of J_z in the Rashba case and of $L_z - S_z$ in the Dresselhaus one reduce the Hamiltonian to block-diagonal form when either is turned off. In these cases, each block describes the Hamiltonian of a two-level system that involves the states $|\ell, \sigma\rangle$ and either $|\ell \pm 2\sigma, \bar{\sigma}\rangle$, depending on whether the

(a) $\cdots \overset{\alpha/a}{\longleftrightarrow} (\ell-2\sigma,\bar{\sigma}) \overset{\beta/a}{\longleftrightarrow} (\ell,\sigma) \overset{\alpha/a}{\longleftrightarrow} (\ell+2\sigma,\bar{\sigma}) \overset{\beta/a}{\longleftrightarrow} \cdots$

(b) $\cdots \overset{\alpha/a}{\longleftrightarrow} (\ell-2\bar{\sigma},\sigma) \overset{\beta/a}{\longleftrightarrow} (\ell,\bar{\sigma}) \overset{\alpha/a}{\longleftrightarrow} (\ell+2\bar{\sigma},\sigma) \overset{\beta/a}{\longleftrightarrow} \cdots$

FIG. 1. Schematic diagram showing how the spin-orbit interactions couple the states $\{|\ell,\sigma\rangle\}$, forming two unconnected chains. In each, every state is linked to two adjacent others with which it shares the same $\langle J_z\rangle$ or $\langle L_z - S_z\rangle$. When one interaction is turned off, the chains split into collections of independent pairs of states (two-level systems) with either definite J_z (if $\beta = 0$) or $L_z - S_z$ (if $\alpha = 0$). The chains **A** and **B** may be constructed by applying the Hamiltonians H_R and H_D alternately on any state $|\ell,\sigma\rangle$. They remain disjoint during time evolution even when both H_R and H_D are present.

conserved quantity is J_z or $L_z - S_z$, respectively. If only one interaction is present, then an arbitrary one-electron state can be interpreted as a superposition of states belonging to different two-level systems that are dynamically independent from one another. This independence is lost when both interactions act simultaneously. In this situation, the state $|\ell,\sigma\rangle$ couples to both $|\ell \pm 2\sigma,\bar{\sigma}\rangle$, and thus effectively connects the two-level systems $\{|\ell,\sigma\rangle, |\ell\pm 2\sigma,\bar{\sigma}\rangle\}$ together. Notice that the three states $|\ell,\sigma\rangle$ and $|\ell\pm 2\sigma,\bar{\sigma}\rangle$ all gain the same global phase under R, since either they share the same J_z eigenvalue or differ in it by an even multiple of $\hbar$. This latter condition defines, in fact, the set of all J_z eigenstates that transform similarly under R. The SOI can therefore only couple such states. As there is nothing special about $|\ell,\sigma\rangle$, the same may be said about, for instance, the states $|\ell\pm 2\sigma,\bar{\sigma}\rangle$. Following this reasoning, the structure of the effective Hamiltonian in the general case may be described schematically as in Fig. 1, by rearranging the J_z eigenstates into two separate chains. Notice that states in different chains differ in their J_z eigenvalue by an odd multiple of $\hbar$. This diagram can be constructed by alternately applying the operators H_R and H_D on any $|\ell,\sigma\rangle$. The symmetry operation R therefore splits the basis states into two groups (the chains in Fig. 1) that remain unconnected during time evolution.

A. Single spin-orbit interaction

Let us concentrate on the dynamics of an electron in the presence of either the Rashba or the Dresselhaus interaction. The results of this section can be obtained analytically, and as such provide also some basic insights into the many-electron dynamics and its conserved quantities. We will consider first an electron in a J_z eigenstate that can only make transitions between states of a two-level system with either definite J_z or $L_z - S_z$ (see Fig. 1). This choice of initial state serves the purpose of simplifying conceptually the analysis. Nevertheless, such state can be prepared with high fidelity by applying an external magnetic field in the z direction and transferring orbital angular momentum to the electron via optical excitation with twisted light [37]. Additionally, in the case of Rashba SOI, this interaction can be controlled and quenched to some extent with an applied voltage [38]. This feature could be used to facilitate the preparation of the initial state. Afterwards, we will relax this choice of initial state in order to analyze the transfer between OAM and SAM in more general terms.

As is well known, the time-evolution operator for an arbitrary two-level system can be computed exactly. If the basis of states spanning the two-level system considered is $\{|\ell,\sigma\rangle, |\ell+2\epsilon_{R,D}\sigma,\bar{\sigma}\rangle\}$, where $\epsilon_R = 1$ for the Rashba interaction and $\epsilon_D = -1$ for the Dresselhaus one, then the operators $U_{R,D}(t)$ are

$$U_{R,D}(t) = e^{-i[(\ell+\epsilon_{R,D}\sigma)^2+1/4]\omega_0 t}[\cos(\vartheta_{R,D}t) - i\Omega_{R,D}\sin(\vartheta_{R,D}t)], \tag{5}$$

where $\omega_0 = E_0/\hbar$, $\vartheta_{R,D} = \sqrt{\omega_0^2+\omega_{R,D}^2}|\ell+\epsilon_{R,D}\sigma|$, $\Omega_R = (\omega_R\sigma_x - 2\sigma\omega_0\sigma_z)(\ell+\sigma)\vartheta_R^{-1}$, and $\Omega_D = -2\sigma(\omega_D\sigma_y - \omega_0\sigma_z)(\ell-\sigma)\vartheta_D^{-1}$. Notice that the transition frequencies $\vartheta_{R,D}$ are respectively proportional to the absolute value of the total angular momentum and of the eigenvalue $\ell-\sigma$ of the operator $L_z - S_z$. They are also invariant under the transformation $(\ell,\sigma)\to(-\ell,-\sigma)$. This last property is related to the time-reversal invariance of the full Hamiltonian. While the operators $\Omega_{R,D}$ depend thus on ℓ and σ, it can be inferred from Eq. (5) that the absolute values of the transition amplitudes are independent of both, and remain limited to

$$|\langle\ell,\sigma|\Omega_{R,D}|\ell+2\epsilon_{R,D}\sigma,\bar{\sigma}\rangle| = \frac{\omega_{R,D}}{\sqrt{\omega_{R,D}^2+\omega_0^2}}. \tag{6}$$

This is seen graphically in Fig. 2, where we pick a pair of H_0 eigenstates for each SOI and compare the time evolution of their occupation probabilities. An electron excited initially into a pure state $|\ell,\sigma\rangle$ will therefore exchange back and forth a maximum of $\hbar\omega_{R,D}^2/(\omega_0^2+\omega_{R,D}^2)$ between OAM and SAM, regardless of its initial OAM. In experimentally feasible cases with typical values for the SOI couplings, this amount is enough to observe a macroscopic change in the electron's spin orientation. As an example, consider a GaAs QR ($m^* = 0.063\,m_e$) of radius $a = 50$ nm and a Rashba coupling of $\alpha = 10.8$ meV nm. In this case $\hbar\omega_R^2/(\omega_0^2+\omega_R^2) \approx 0.44\hbar \approx \hbar/2$. What helps the SOI induce such a noticeable change in the spin orientation is the close confinement of the electron in this particular geometry, which essentially restricts the in-plane momentum to $k_\parallel = k_\varphi = L_z/a\hbar$. An electron can therefore change its momentum only by changing its OAM. In particular, transitions between adjacent energy levels imply gaining or losing a unit of $\hbar$. Furthermore, the conservation of either J_z (if $\beta = 0$) or $L_z - S_z$ (if $\alpha = 0$) forces the spin to adapt, especially to such significant changes. Notice that, compared to the usual quasi-2D quantum well [39], the energy and momentum scales are not too different in this case for electrons in the lower end of the spectrum (small $|\ell|$). The effect of the annular confinement manifests itself instead in the eigenstates of $H_{R,D}$, which in our case gives rise to a nonvanishing $\langle S_z\rangle$ [14,17,28]. This first result is by itself significant in our search of control tools for the transfer of angular momentum from orbital to spin degrees of freedom, the latter being the one that mediates the interaction between charge carriers and doped magnetic impurities. Indeed, it is telling us that a significant transfer between orbital and spin angular momentum is perfectly attainable in semiconductor structures via both spin-orbit interactions. Also, regarding the coherent-control goal, we remark on the independence of the amplitude of the oscillations in Fig. 2 with respect to ℓ. In

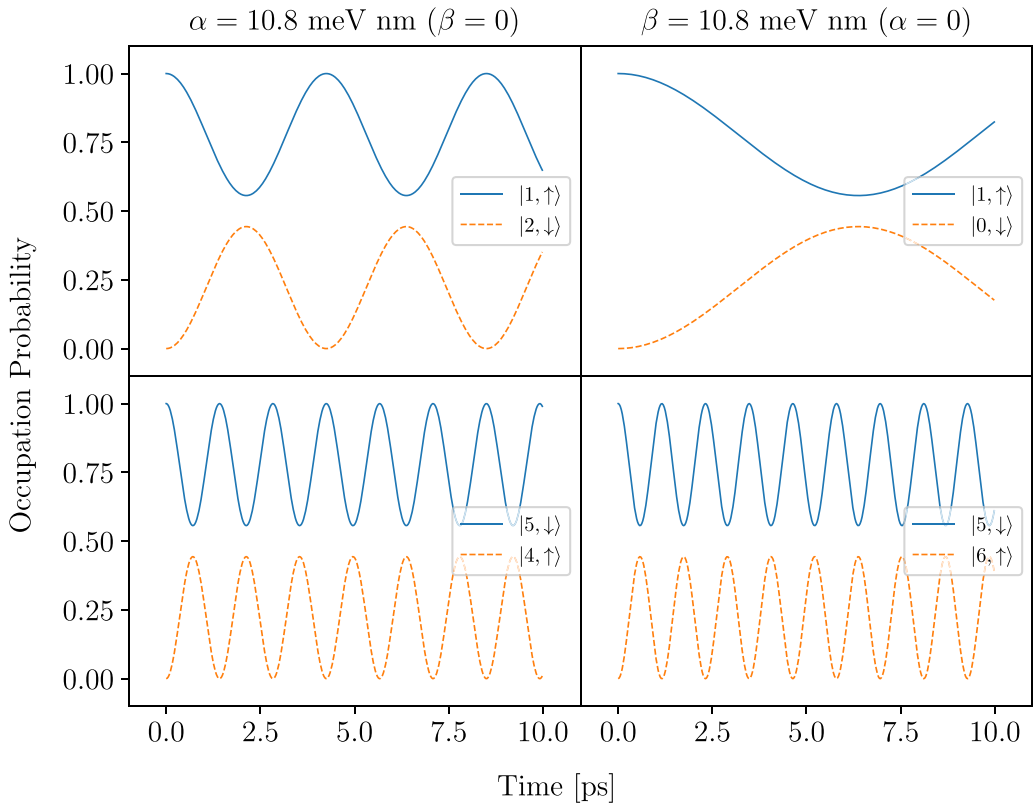

FIG. 2. Time evolution of the occupation probabilities under the action of the Rashba (left column) and Dresselhaus (right column) interactions for an electron initially in two different H_0 eigenstates. We consider for these calculations a GaAs QR ($m^* = 0.063m_e$) of radius $a = 50$ nm. For typical values of α and β, the SAM converted into OAM in one cycle is significant (nearly 50% of the initial spin polarization), and independent of the electron's energy, as higher energy ones (i.e., those of higher $|\ell|$) have the same transition amplitudes as their lower energy counterparts.

this sense the importance of ℓ rests on the sensitive frequency of the oscillations, which should provide enough time for the exchange interaction between electron and impurity spins to take place. On the other hand, a higher frequency of the oscillations between OAM and SAM (obtained by choosing a higher value of ℓ) might be desirable in contexts where the control dynamics needs to be accelerated to overcome decoherence.

Let us now consider an electron initially in a more general state

$$|\psi\rangle = \sqrt{\tfrac{1}{2} + p}\ |\ell, \uparrow\rangle + e^{i\phi}\sqrt{\tfrac{1}{2} - p}\ |\ell + \epsilon_{R,D}, \downarrow\rangle, \quad (7)$$

with $|p| \leqslant 1/2$, which corresponds to an initial spin polarization of $\langle\psi|S_z|\psi\rangle = \hbar p$. A discussion of the possible strategies to prepare this initial state is beyond the scope of this work, but the reader may consult available quantum control strategies like, for example, the ones considered in Ref. [40]. In Fig. 3 we vary the relative phase $e^{i\phi}$ and the polarization p to study how the maximum angular momentum exchanged varies with the initial state. To do this, we let the system evolve under $U_{R,D}(t)$ and compute the maximum deviation of $\langle S_z\rangle(t)$ with respect to $\hbar p$, which occurs for some $0 \leqslant t < 2\pi/\vartheta_{R,D}$ in a cycle. We remark that, as before, this amount does not depend on ℓ at all (see Appendix B). The results of Fig. 3 are meant to guide possible control strategies leading to a maximum transfer between OAM and SAM, and thereby to a more efficient exchange interaction between the electron and magnetic impurities added to the QR.

The above results for a single electron can be used to draw conclusions regarding the angular momentum dynamics in many-electron Slater determinants. Some essential aspects of the behavior of the system as a whole can be inferred just by inspecting how the electrons are initially distributed on the chains in Fig. 1, without resorting to numerical computations. As a simple example, consider two electrons occupying initially the states $|\ell, \sigma\rangle$ and $|-\ell, \bar{\sigma}\rangle$. The total OAM and SAM vanish permanently for this configuration. This stems directly from the conservation of $\langle J_z\rangle$ or $\langle L_z - S_z\rangle$ for each electron, and physically it is related to the fact that one spin precesses with the same frequency as the other, due to time-reversal invariance, but in the opposite direction, and thus their contributions to the total $\langle S_z\rangle$ cancel out.

B. Simultaneous Rashba and Dresselhaus interactions

When both spin-orbit interactions are present the separation in two-level systems is lifted (see Fig. 1). Then, in principle, an electron initially in an eigenstate of H_0 can visit all the states in its chain (transitions between chains **A** and **B** are still forbidden). In practice, however, for timescales of processes like optical excitation of carriers with twisted light [41,42] and their interaction with impurities in diluted magnetic semiconductors [43,44], even when a SOI is taken

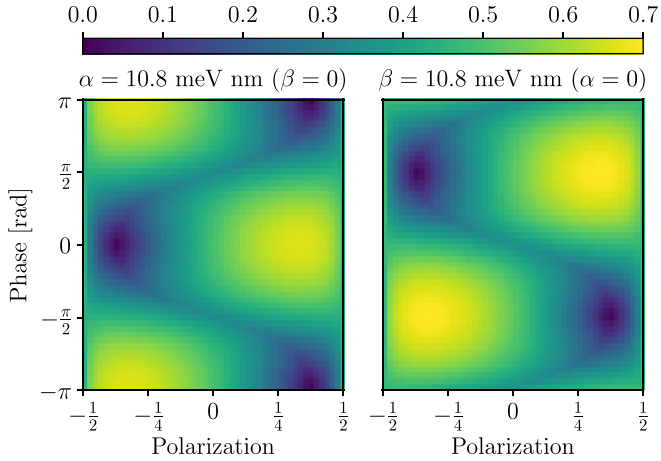

FIG. 3. Maximum deviation (in units of $\hbar$) of the electron's SAM from its initial polarization p, $\max_{0\leqslant t<2\pi\vartheta_{R,D}^{-1}} |\hbar^{-1}\langle S_z\rangle(t) - p|$, as a function of its initial state $|\psi\rangle$, which we express parametrically as $|\psi\rangle = \sqrt{1/2+p}\,|\ell,\uparrow\rangle + e^{i\phi}\sqrt{1/2-p}\,|\ell+\epsilon_{R,D},\downarrow\rangle$, with $e^{i\phi}$ a relative phase. The ring parameters are the same as those in Fig. 2. The centers of the purple puddles correspond to eigenstates of the two-level system, for which as expected no change in the polarization is observed. In contrast, the largest deviations ($0.7\hbar > \hbar/2$) correspond to symmetric and antisymmetric combinations of these eigenstates. The deviation observed in most cases indicates that the change induced by the SOI in the electron's polarization is macroscopic.

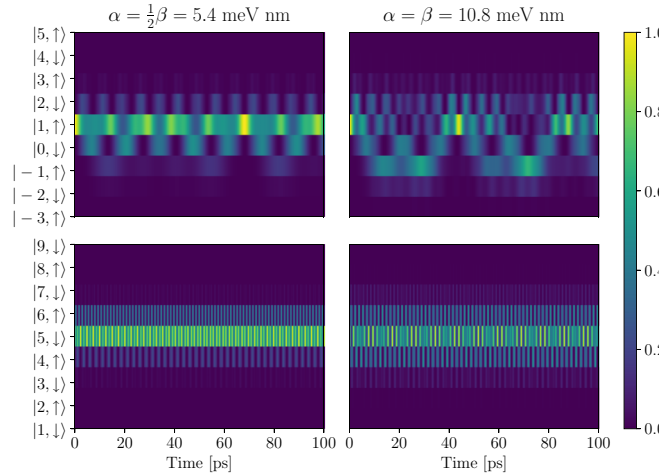

FIG. 4. Occupation probability over time for an electron initially in $|1,\uparrow\rangle$ (top row) and $|5,\downarrow\rangle$ (bottom row), for fixed Dresselhaus and two different Rashba coupling constants. Here it is seen that the initial wave function does not spread beyond the first few neighboring states, even for large α. Also, the extent of the spread is similar for both initial states, as suggested by Eq. (8).

into account [45], we find that the wave function of such an electron does not spread beyond the first few neighbors of the initial state. This is a consequence of the fact that, for experimentally feasible QRs with typical values for α and β, the matrix elements of the SOI Hamiltonian connecting adjacent states are proportional to but smaller than the energy difference between them [see Eqs. (3) and (4)]. This is an important conclusion in the search for control strategies of the angular momenta in QRs.

Let us roughly estimate the extent of the departure from an initial state $|\ell,\sigma\rangle$ caused by the Rashba and Dresselhaus SOI. In order to simplify the discussion, let us assume $\alpha, \beta/2aE_0 \ll 1$, so that spectrum and eigenstates of H do not differ significantly from those of H_0. On this assumption, energy conservation and the existence of a ground state together limit the spread of the initial wave function over states of larger OAM. We can estimate this limit by approximating the first nonvanishing contribution to the probability amplitude of transitioning to a state $|\ell+2k\sigma,(-1)^k\sigma\rangle$ ($k\neq 0$) on the same chain as $|\ell,\sigma\rangle$, using time-dependent perturbation theory. This contribution is of order $|k|$ in the SOI coupling constants. For our purposes, it suffices to take into account only those transitions that do not invert the OAM sign, since states of OAM differing only in sign are degenerate and energetically above the ground state, which in this case corresponds to the (perturbed) state of OAM $\ell+2k\sigma=0$. Assuming, then, that $\ell(\ell+2k\sigma)\geqslant 0$, we obtain

$$|\langle \ell+2k\sigma,(-1)^k\sigma|U(t)|\ell,\sigma\rangle| \approx 2\left(\frac{\alpha\beta}{4a^2E_0^2}\right)^{|n|}\left[\delta_{m,0}+\frac{\alpha}{2aE_0}\delta_{m,1}+\frac{\beta}{2aE_0}\delta_{m,-1}\right], \quad (8)$$

where we write $k=2n+m$ (with n,m integers satisfying $nm\geqslant 0$ and $m=-1,0,1$). Let us now consider the same QR as in Fig. 2, for which $E_0\approx 0.24$ meV, and $\alpha=\beta=10.8$ meV nm ($\alpha,\beta/a\approx 0.216$ meV). Following Eq. (8), we expect the first $|k|<3$ adjacent states to $|\ell,\sigma\rangle$ to have a significant probability of being occupied.

Figure 4 shows exact numerical results that validate the previous perturbative analysis, for evolution under joint Dresselhaus ($\beta=10.8$ meV nm) and Rashba SOIs ($\alpha=\beta/2,\beta$). As in Fig. 2, we consider two initial states, $|1,\uparrow\rangle$ and $|5,\downarrow\rangle$. We plot the occupation probability over time and we see that the initial wave function does not spread beyond the first few neighboring states, even for a large coupling constant α and long times. Note that the extent of the spread is similar for both initial states in spite of their very different values of OAM, as suggested by Eq. (8), similarly to what we saw in Fig. 2. These findings also bear on the design of possible control methods to manipulate the OAM and SAM of carriers via the SOIs.

In physical terms, the above analysis indicates that the change in the electron's total angular momentum is restricted to $|\Delta J_z|\leqslant 2\hbar|n-\delta_{m,-1}|$. We mention here again that, additionally, transitions to states $|\ell+2\sigma k,(-1)^{k+1}\sigma\rangle$ are not possible since these belong to the chain uncoupled from that of $|\ell,\sigma\rangle$. A practical consequence of these results is that the dynamics of an electron in a more complex initial state could also be accurately described using a reduced (finite-dimensional) Hamiltonian.

With the help of Figs. 5 and 6 we now analyze in more detail the exact evolution of the occupation of neighboring states for the same pair of initial states as in Fig. 2, with Rashba and Dresselhaus SOIs present. We consider $\beta=10.8$ meV nm and three values of the Rashba coefficient: $\alpha=\beta/2,\beta,2\beta$.

In Fig. 5 we take $|1,\uparrow\rangle$ as initial state, that is, a low value of OAM, $\ell=1$. In the top panel we have the smallest

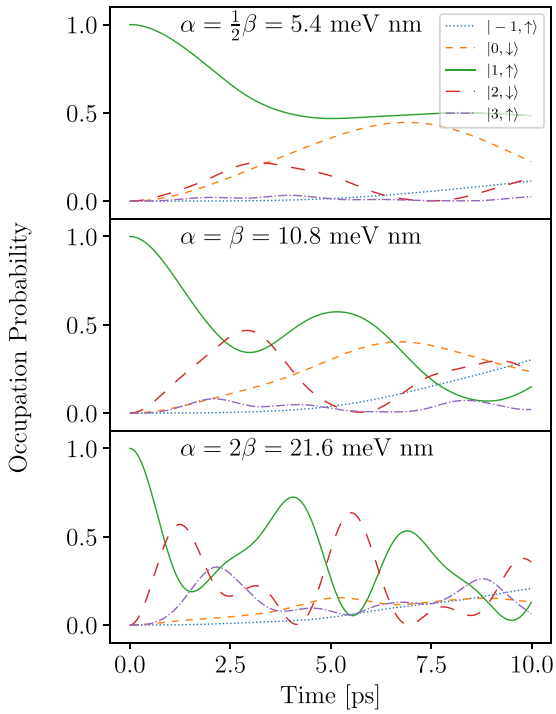

FIG. 5. Occupation probability over time for an electron initially in the pure state $|1,\uparrow\rangle$ of a GaAs ($m^* = 0.063m_e$) QR of radius $a = 50$ nm. Notice that the occupation of the second-nearest neighbor state $|-1,\uparrow\rangle$ reaches 30% only when Rashba coupling is large enough ($\alpha/a \gtrsim E_0 \approx 0.24$ meV). That the optimal configuration is $\alpha = \beta$ in this case is related to the fact that transitions from $|0,\downarrow\rangle$ into and out of this state have the same probability.

value of α, equal to $\beta/2$. Nevertheless, the occupation of the initial state $|1,\uparrow\rangle$ (green solid line) drops significantly to about 50%. Most of the occupation goes to the neighboring Dresselhaus-connected $|0,\downarrow\rangle$ state (short-dashed orange line). Also the transfer to the neighboring Rashba-connected $|2,\downarrow\rangle$ state (long-dashed red line) is significant. The state $|-1,\uparrow\rangle$ (dotted blue line) increasingly draws occupation from $|0,\downarrow\rangle$ via Rashba SOI, as a second order, Dresselhaus plus Rashba effect. The other second-nearest neighbor state, $|3,\uparrow\rangle$ (dash-dotted violet line), clearly remains less populated in this time window of 10 ps. Thus we see that the evolution remains largely confined to this group of five neighboring states centered around and including the initial state. In the middle panel of Fig. 5 we have $\alpha = \beta$. Here the stronger Rashba coupling causes the state $|2,\downarrow\rangle$ to compete advantageously with the state $|0,\downarrow\rangle$, and both states together drain almost completely the occupation out of the initial state by $t \approx 8$ ps. The second-nearest neighbor states also start to play a more significant role, but still the occupation of these five states combined adds up roughly to one at all times (not shown). Finally, in the bottom panel of Fig. 5 we have a strong Rashba coupling of $\alpha = 2\beta$. Here the occupation of the initial state $|1,\uparrow\rangle$ suffers multiple strong changes and the Rashba-coupled first neighbor $|2,\downarrow\rangle$ plays a central role. In particular, it rapidly feeds the occupation of $|3,\uparrow\rangle$ via their Dresselhaus connection. By the final time of $t \approx 10$ ps a fairly complex scenario is reached, where all five states are similarly occupied.

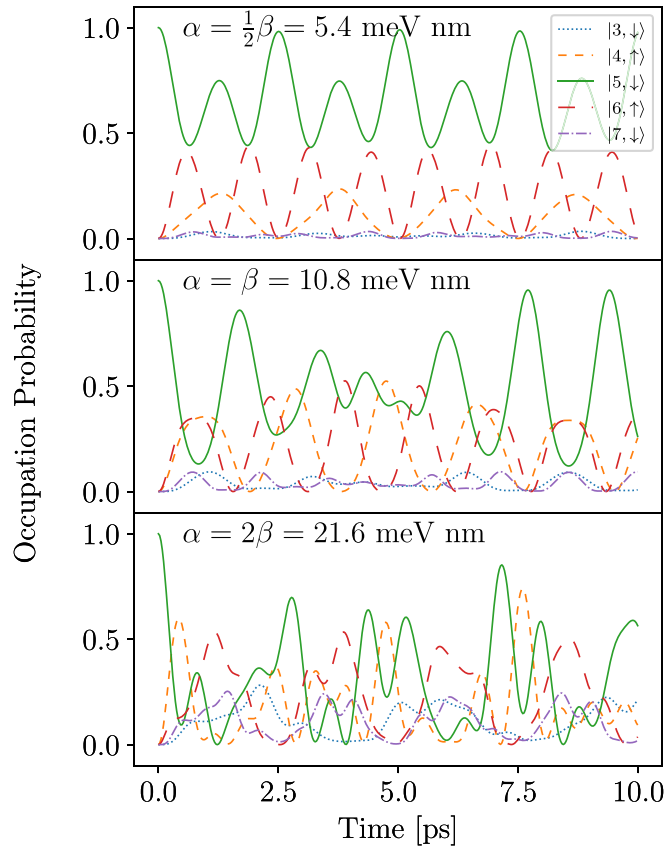

FIG. 6. Occupation probability over time for an electron initially in the pure state $|5,\downarrow\rangle$. The ring parameters are the same as in Fig. 5. Again, only for large Rashba couplings is there a considerable occupation of the second-nearest neighbor states, $|3,\downarrow\rangle$ and $|7,\uparrow\rangle$. In contrast to the transition frequencies, these probabilities do not differ significantly from their counterparts in the case $|1,\uparrow\rangle$ in Fig. 5. This is in line with the bound in Eq. (8), which shows that their dependence on ℓ cannot be too strong.

In Fig. 6 we present analogous results for $|5,\downarrow\rangle$ as initial state, this time with a high value of OAM, $\ell = 5$. As remarked earlier, for higher values of ℓ the whole dynamics becomes more rapid, but the effects on the amplitudes of the various occupations remain similar to the $\ell = 1$ case. Again we see that as the Rashba constant α increases, the exchange of populations becomes more fluid and evenly shared among the initial state and its two first-nearest neighbors in the chain. Since the high value of $\ell = 5$ accelerates the dynamics, these results allow us to see a (relatively speaking) bigger time window of evolution. Even for the strongest Rashba coupling we see nevertheless that the occupation remains largely confined in the restricted group of five states including the initial state. In other words, we see a sort of localization in spite of the strong and influential Rashba and Dresselhaus SOIs.

IV. INFLUENCE OF EXCITED RADIAL STATES

Let us now study how the inclusion of an excited radial state influences the dynamics of the observables studied in Secs. II and III. To this end, we will consider in this section the model developed by Shakouri *et al.* [13], which offers a

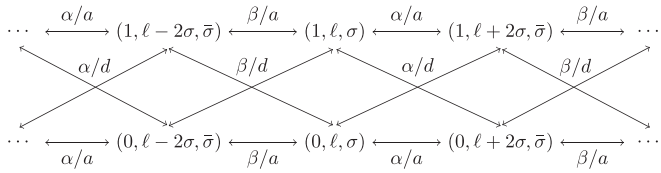

FIG. 7. Ladder **A** of states connected by the Hamiltonian in the Shakouri *et al.* model. Notice that the addition of an excited radial mode in this model is completely transparent to the action of R, and then ladders **A** and **B** (**B** not shown) remain disjoint during the time evolution, as did chains **A** and **B** in the Meijer *et al.* model. (The states shown in this figure all gain the same global phase when rotated by R.) For very narrow QRs ($d/a \ll 1$), as considered by the authors (where $d/a \approx 1/8$ in [13]), inter-RM transitions are much faster than intra-RM ones. The rates of the latter are exactly the same as in the Meijer *et al.* model (see Sec. III).

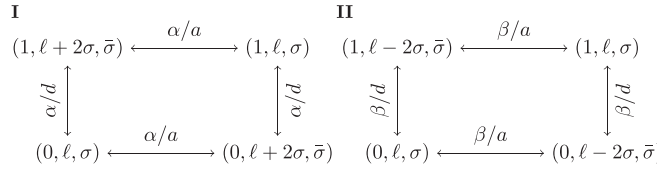

FIG. 8. General diagram of a four-level system making up an independent block in the pure Rashba (**I**) and Dresselhaus (**II**) cases. Inter-RM transitions depend on the width of the ring and the coupling constant only [13], whereas intra-RM ones depend on ℓ and σ but not on n [see Eqs. (3) and (4)].

different treatment of the ring's width while considering the same linear Rashba and Dresselhaus Hamiltonians as in Eq. (2).

The authors assume a narrow QR of effective width d (related to the parameter a_3 in their paper). The eigenstates of H_0 now form an extended basis $\{|n,\ell,\sigma\rangle\}$, where $n = 0, 1$ indicates the radial level. Transitions between basis states will be called inter-radial-mode (inter-RM) and intra-radial-mode (intra-RM) transitions depending on whether n changes or not, respectively. In the absence of an external magnetic field, the ring's width is proportional to $a\sqrt{E_0/\hbar\omega_r}$, where $\hbar\omega_r$ is the strength of the confining potential, which is assumed to be harmonic and isotropic (φ independent). In the effective Hamiltonian now obtained, the intra-RM matrix elements are exactly the same as those deduced in Eqs. (3) and (4). In contrast, inter-RM matrix elements are proportional to $\alpha, \beta/d$, and depend only on the ring's parameters and the SOI coupling constants (and not on ℓ or σ) [13].

As before, the quantities J_z and $L_z - S_z$ are conserved in the pure Rashba and Dresselhaus cases, respectively, even in inter-RM transitions. In the extended basis $\{|n,\ell,\sigma\rangle\}$, the way the full Hamiltonian connects the states can be represented schematically as in Fig. 7. Notice that all the transitions, including the inter-RM ones, involve spin flips, since they are all induced by the SOIs. Also, we point out that each of the disjoint chains **A** and **B** shown in Fig. 1 now becomes a sort of ladder (or double chain). In Fig. 7 we draw only the "ladder **A**" (corresponding to the chain **A**) which contains the states $|n,\ell,\sigma\rangle$ with $n = 0, 1$, and omit the "ladder **B**" which contains the states $|n,\ell,\bar{\sigma}\rangle$. These two ladders remain disjoint during the evolution, like the chains **A** and **B** in the model of Meijer *et al.* The justification for this separation runs as before, now with the unperturbed (without SOIs) Hamiltonian being $H_0 = E_0 L_z^2/\hbar^2 + \hbar\omega_r(N_n + 1/2)$, where N_n gives the occupation of the radial state n. The diagram in Fig. 7 shows that, as before, the absence of one SOI divides the Hamiltonian into a collection of independent blocks, each block consisting now of four states. In Fig. 8 we give the general structure of these blocks for the pure Rashba and Dresselhaus cases.

Let us compare the evolutions computed with the models of Meijer *et al.* and Shakouri *et al.*. To this end, in Fig. 9 we plot the expectation values $\langle L_z\rangle$ and $\langle S_z\rangle$ calculated for six different initial states, i.e., $|n = 0, \ell, \uparrow\rangle$, with $\ell = 0, \ldots, 5$. We consider a narrow GaAs ($m^* = 0.063m_e$) QR of radius $a = 50$ nm and width $d/a \approx 1/8$, with $\beta = 10.8$ meV nm and a large Rashba coupling of $\alpha = 2\beta$. Each row in the figure corresponds to a given initial state, and it includes a plot of the ratio of occupations of the radial states, $\langle N_1\rangle/\langle N_0\rangle$. It is seen that in all cases the occupation of the excited radial state is very low compared to that of the lower state (less than 3%). In spite of that, we find that for low values of ℓ the excited radial state does play an important role in the evolution of $\langle L_z\rangle$ and $\langle S_z\rangle$. Starting at $\ell \approx 3$ and above, the two models produce very similar results, thus favoring the use of the simpler model of Meijer *et al.*.

Three questions arise: Why does the upper radial level remain largely unpopulated for all initial values of ℓ? How can it still affect strongly the dynamics for low ℓ? Why does it become irrelevant for higher ℓ? Essentially the existence of the small upper bound for the occupation $\langle N_1\rangle$ is due to the fact that the inter-RM matrix elements are much smaller than the energy $\hbar\omega_r$ associated to the radial confinement, even for large SOI couplings. The influence of the largeness of $|\ell|$ comes from the fact that the intra-RM matrix elements are proportional to ℓ [see Eqs. (3) and (4)] and become more relevant and eventually dominant for large $|\ell|$ (the inter-RM matrix elements are independent of ℓ). In other words, when the intra-RM transitions become dominant over the inter-RM ones (thanks to a high value of $|\ell|$), the presence of the excited radial level in the model becomes superfluous.

When systems with more than one electron are considered, the inclusion in the model of the second radial state would likely become necessary in general, since Pauli blocking is especially restrictive in effectively one-dimensional situations. We leave that interesting problem for future work.

V. CONCLUSION

We studied the dynamics of a single electron under the action of the Rashba and Dresselhaus spin-orbit interactions in narrow quantum rings. To this end, we considered first the model by Meijer *et al.*, originally developed for very narrow quantum rings with only the Rashba interaction, and then included the extended model worked out by Shakouri *et al.* for narrow but finite-width rings. In the former, only the ground transversal mode is considered, whereas the latter allows for transitions within the ground and first excited transversal modes. When only one SOI is taken into account,

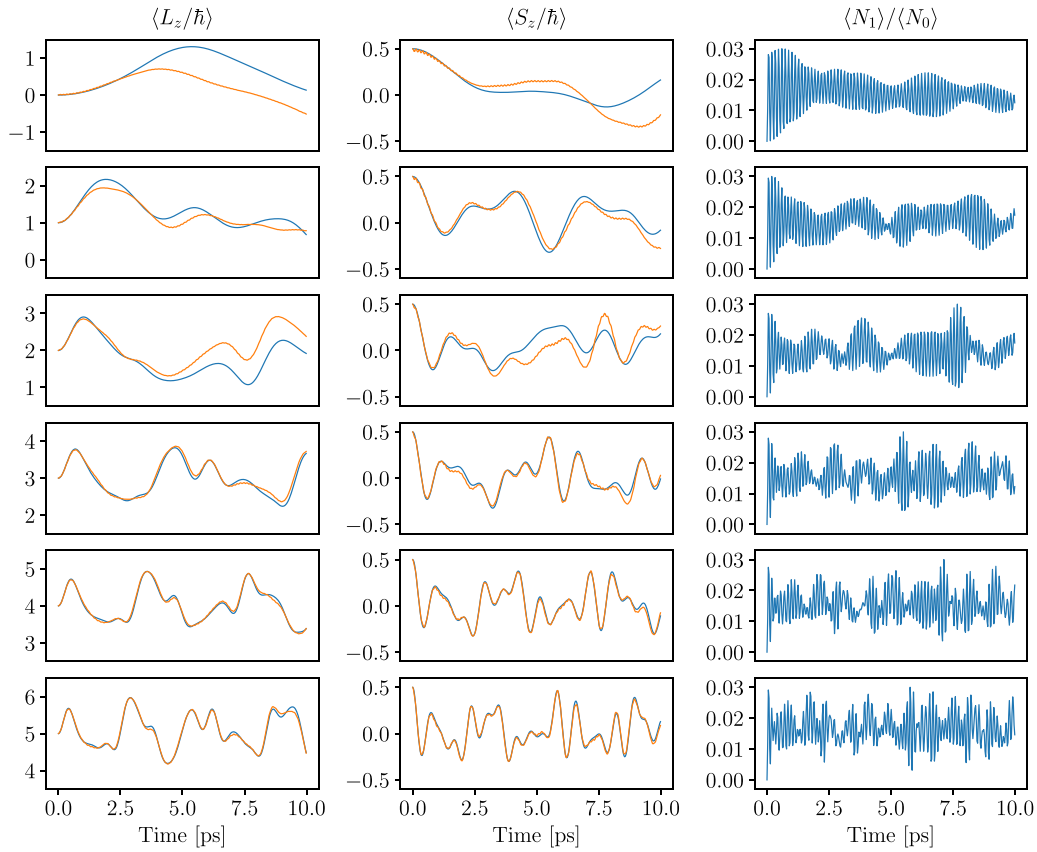

FIG. 9. First two columns: Time evolution of the expectation values $\langle L_z\rangle$ and $\langle S_z\rangle$ for an electron initially in an eigenstate of H_0, $|n = 0, \ell, \uparrow\rangle$, with $\ell = 0, \ldots, 5$. Each row corresponds to a different value of ℓ. Third column: Occupation of the excited radial level relative to the ground level. Following Shakouri *et al.*, we assume a GaAs ring of radius $a = 50$ nm and a parabolic radial confinement that gives an effective ring width of $d \approx a/8$. The SOI coupling constants are $\alpha = 2\beta = 21.6$ meV nm.

a conserved quantity appears (either J_z or $L_z - S_z$) that allows the Hamiltonian to be written in block-diagonal form, where each block is of dimension two, if only one radial mode is considered, or four, if the excited mode is also included. We showed in Sec. II and will show in Appendix A that the conservation of J_z and $L_z - S_z$ is a property of the Rashba and Dresselhaus linear Hamiltonians, independent of any particular approximation. Furthermore, we showed that, if the bare Hamiltonian H_0 conserves J_z, these interactions reduce the symmetry to a rotation by π about the axis of the ring. From the existence of this symmetry we concluded that an effective Hamiltonian that meets the above condition always splits into two independent blocks, even if both interactions are included in the dynamics.

An important result from the point of view of quantum control, presented in Sec. III A, is that for experimentally feasible rings, the presence of one SOI is enough to observe a temporary but macroscopic change in the spin orientation of an initially spin-polarized electron with definite OAM. This macroscopic change is favored by the quasi-one-dimensional geometry.

The calculations and analysis presented here are meant as a stepping stone towards the goal of controlling the angular momentum of light, charge carriers, and magnetic impurities in nanostructures. Photoexcitation with optical vortices carrying orbital angular momentum and the exchange interaction between the electron spin and magnetic impurities are two other important elements towards the optical control of magnetic impurities. Here we have explored the effectiveness of the Rashba and Dresselhaus spin-orbit interactions to produce a significant and rapid interchange between orbital and spin angular momenta for the charge carriers. Also we examined in detail the diffusion of the occupation from an initial state with well-defined spin and orbital angular momentum, and found that it is fairly limited and insensitive to the initial value of orbital angular momentum in realistic systems. In other words, large changes in orbital angular momentum are not to be expected through the action and Rashba and Dresselhaus spin-orbit interactions.

Quasi-1D quantum rings are only one example of nanostructures in which quantum control of information-holding variables holds promise to be implemented. Different types of quantum dots are also classic candidates in this sense. An approach to these important systems, and also perhaps a more realistic treatment for existing quantum rings, consists of relaxing the strict quasi-1D nature of the our ring model. For this reason, in Sec. IV we studied rings with two radial modes, following the model of Shakouri *et al.* By monitoring the mean values of the orbital and spin angular momenta, we found that, for high values of the initial OAM, the model of Meijer *et al.* captures accurately the evolution. On the other hand, large discrepancies appear for low initial OAM between

the two models. This limitation of the simpler model ought to be taken into account when modeling the quantum control of states of even single electrons. We speculate that in the presence of more than one electron the second radial level would become necessary even for high values of the initial OAM due to the influence of Pauli blocking and Coulomb repulsion.

ACKNOWLEDGMENTS

We acknowledge financial support from the University of Buenos Aires Grant No. UBACyT 2018-20020170100711BA, and from the Argentine ANPCyT, Grant No. PICT-2016-1056.

APPENDIX A: CONSERVATION OF J_z AND $L_z - S_z$

We wish to show that $[H_R, J_z] = [H_R, L_z + S_z] = [H_D, L_z - S_z] = 0$. Because $[L_z, S_z] = [L_z, \sigma_\pm] = 0$, this reduces to computing the commutators $[k_\pm, L_z]$ and $[\sigma_\pm, S_z]$, and showing that $[H_R, L_z] = -[H_R, S_z]$ and that $[H_D, L_z] = [H_D, S_z]$. As it is not hard to show that $[\sigma_\pm, S_z] = \mp\sigma_\pm$, we will concentrate only on the commutators $[k_\pm, L_z]$.

The general form of the operators $k_\pm$ in cylindrical-polar coordinates is

$$k_\pm = k_x \pm ik_y = -ie^{\pm i\varphi}\left[\partial_r \pm \frac{i}{r}\partial_\varphi\right]. \tag{A1}$$

Given that $L_z = -i\hbar\partial_\varphi$, the commutators $[k_\pm, \partial_\varphi] = i\hbar^{-1}[k_\pm, L_z]$ are

$$\begin{aligned}[k_\pm, \partial_\varphi] &= k_\pm\partial_\varphi - \partial_\varphi k_\pm \\ &= k_\pm\partial_\varphi + i(\pm ie^{\pm i\varphi} + e^{\pm i\varphi}\partial_\varphi)\left[\partial_r \pm \frac{i}{r}\partial_\varphi\right] = \mp ik_\pm.\end{aligned} \tag{A2}$$

Therefore,

$$\begin{aligned}[H_R, L_z] &= i\alpha([k_-, L_z]\sigma_+ - [k_+, L_z]\sigma_-) = i\alpha\hbar(k_-\sigma_+ + k_+\sigma_-) \\ &= -i\alpha\hbar[k_-(-\sigma_+) - k_+\sigma_-] \\ &= -i\alpha\hbar(k_-[\sigma_+, S_z] - k_+[\sigma_-, S_z]) = -[H_R, S_z].\end{aligned} \tag{A3}$$

Similarly, for the commutator $[H_D, L_z - S_z]$ we have

$$\begin{aligned}[H_D, L_z] &= \beta([k_+, L_z]\sigma_+ + [k_-, L_z]\sigma_-) = \hbar\beta(k_-\sigma_- - k_+\sigma_+) \\ &= \hbar\beta[k_-\sigma_- + k_+(-\sigma_+)] \\ &= \hbar\beta(k_-[\sigma_-, S_z] + k_+[\sigma_+, S_z]) = [H_R, S_z].\end{aligned} \tag{A4}$$

APPENDIX B: INDEPENDENCE OF THE EXTREMA OF $\langle S_z\rangle(t)$ FROM ℓ IN THE PURE RASHBA AND DRESSELHAUS CASES

In order to make the analysis clearer, in this Appendix we consider only the Rashba case; an analogous argument applies to the Dresselhaus case. Let us consider the time-dependent state $|\psi(t)\rangle \equiv U_R(t)|\psi\rangle$, where $|\psi\rangle = |\psi(0)\rangle$ is the initial state defined in Eq. (7) for the Rashba case (recall that $\epsilon_R = 1$). We wish to show that the extrema of $\langle\psi(t)|S_z|\psi(t)\rangle$ do not depend on ℓ. The expectation value of S_z taken with respect to $|\psi(t)\rangle$ can be written as

$$\begin{aligned}\langle\psi(t)|S_z|\psi(t)\rangle = {}& \langle\psi|S_z|\psi\rangle\cos^2(\vartheta_R t) \\ &+ \langle\psi|i[\Omega_R, S_z]|\psi\rangle\cos(\vartheta_R t)\sin(\vartheta_R t) \\ &+ \langle\psi|\Omega_R S_z\Omega_R|\psi\rangle\sin^2(\vartheta_R t).\end{aligned} \tag{B1}$$

It follows from Eq. (B1) that the expectation value $\langle\psi(t)|S_z|\psi(t)\rangle$ attains its extrema at times $\vartheta_R t$ that satisfy the condition

$$\begin{aligned}\tan(2\vartheta_R t) &= \frac{\langle\psi|i[\Omega_R, S_z]|\psi\rangle}{\langle\psi|S_z|\psi\rangle - \langle\psi|\Omega_R S_z\Omega_R|\psi\rangle} \\ &= \frac{\hbar\langle\psi|\sigma_y|\psi\rangle\sqrt{\omega_0^2 + \omega_R^2}}{2\omega_R\langle\psi|S_z|\psi\rangle + \hbar\omega_0\langle\psi|\sigma_x|\psi\rangle}\,\frac{\ell + 1/2}{|\ell + 1/2|}.\end{aligned} \tag{B2}$$

The right-hand side of Eq. (B2) depends on the sign of $\ell + 1/2$, which coincides with that of ℓ if $\ell \neq 0$. It can be shown by direct computation that this dependence comes solely from the numerator $\langle\psi|i[\Omega_R, S_z]|\psi\rangle$, because the quantities $\langle\psi|S_z|\psi\rangle$ and $\langle\psi|\Omega_R S_z\Omega_R|\psi\rangle$ do not depend on ℓ at all. By properly inverting the relation in Eq. (B2) and substituting the result for $\vartheta_R t$ into Eq. (B1), it can be shown that each term of the latter is independent of the sign of $\ell + 1/2$. Choosing a particular ℓ therefore sets the sign of $\ell + 1/2$ and the frequency ϑ_R, and thus affects the location of each extremum, but has no effect on their amplitudes. We conclude that all the extrema of $\langle\psi(t)|S_z|\psi(t)\rangle$ are independent of ℓ.

[1] R. Winkler, *Spin-Orbit Coupling in Two-Dimensional Electron and Hole System* (Springer Verlag, Berlin Heidelberg, 2003), Vol. 191.
[2] M. I. Dyakonov, *Spin Physics in Semiconductors*, Solid-State Sciences (Springer, New York, 2008).
[3] S. Bandyopadhyay and M. Cahay, *Introduction to Spintronics* (CRC Press, Boca Raton, FL, 2016).
[4] M. Wu, J. Jiang, and M. Weng, Phys. Rep. **493**, 61 (2010).
[5] Yu. A. Bychkov and E. I. Rashba, JETP Lett. **39**, 78 (1984).
[6] N. B. Clayburn, J. L. McCarter, J. M. Dreiling, M. Poelker, D. M. Ryan, and T. J. Gay, Phys. Rev. B **87**, 035204 (2013).
[7] M. Cygorek, P. I. Tamborenea, and V. M. Axt, Phys. Rev. B **92**, 115301 (2015).
[8] L. Jacak, P. Hawrylak, and A. Wójs, *Quantum Dots* (Springer, New York, 1998).
[9] L. Bányai and S. W. Koch, *Semiconductor Quantum Dots* (World Scientific, Singapore, 1993).
[10] V. M. Fomin, *Physics of Quantum Rings*, NanoScience and Technology (Springer, New York, 2014).
[11] G. Dresselhaus, Phys. Rev. **100**, 580 (1955).
[12] F. E. Meijer, A. F. Morpurgo, and T. M. Klapwijk, Phys. Rev. B **66**, 033107 (2002).

[13] K. Shakouri, B. Szafran, M. Esmaeilzadeh, and F. M. Peeters, Phys. Rev. B **85**, 165314 (2012).
[14] D. Frustaglia and K. Richter, Phys. Rev. B **69**, 235310 (2004).
[15] G. S. Lozano and M. J. Sánchez, Phys. Rev. B **72**, 205315 (2005).
[16] M. P. Nowak and B. Szafran, Phys. Rev. B **80**, 195319 (2009).
[17] B. Berche, C. Chatelain, and E. Medina, Eur. J. Phys. **31**, 1267 (2010).
[18] G. F. Quinteiro, P. I. Tamborenea, and J. Berakdar, Opt. Express **19**, 26733 (2011).
[19] F. K. Joibari, Y. M. Blanter, and G. E. W. Bauer, Phys. Rev. B **90**, 155301 (2014).
[20] A. Zamani, F. Setareh, T. Azargoshasb, and E. Niknam, Superlattices Microstruct. **115**, 40 (2018).
[21] S. E. Pourmand and G. Rezaei, Phys. B: Condens. Matter **543**, 27 (2018).
[22] V. K. Kozin, I. V. Iorsh, O. V. Kibis, and I. A. Shelykh, Phys. Rev. B **97**, 155434 (2018).
[23] A. Hijano, T. L. van den Berg, D. Frustaglia, and D. Bercioux, Phys. Rev. B **103**, 155419 (2021).
[24] S. Peng, F. Ouyang, W. Luo, and T. Chakraborty, Phys. E **128**, 114545 (2021).
[25] T. Kuroda, T. Mano, T. Ochiai, S. Sanguinetti, K. Sakoda, G. Kido, and N. Koguchi, Phys. Rev. B **72**, 205301 (2005).
[26] S. Gumber, M. Gambhir, P. K. Jha, and M. Mohan, J. Appl. Phys. **119**, 073101 (2016).
[27] J. S. Sheng and K. Chang, Phys. Rev. B **74**, 235315 (2006).
[28] J. M. Lia and P. I. Tamborenea, Phys. E **126**, 114419 (2021).
[29] K. D. Greve, D. Press, P. L. McMahon, and Y. Yamamoto, Rep. Prog. Phys. **76**, 092501 (2013).
[30] A. Greilich, S. G. Carter, D. Kim, A. S. Bracker, and D. Gammon, Nat. Photonics **5**, 702 (2011).
[31] J. Wätzel, E. Y. Sherman, and J. Berakdar, Phys. Rev. B **101**, 235304 (2020).
[32] X. Wang, Z. Nie, Y. Liang, J. Wang, T. Li, and B. Jia, Nanophotonics **7**, 1533 (2018).
[33] U. C. Mendes, M. Korkusinski, and P. Hawrylak, Phys. Rev. B **89**, 195308 (2014).
[34] T. Dietl and H. Ohno, Rev. Mod. Phys. **86**, 187 (2014).
[35] G. F. Koster, J. O. Dimmock, R. G. Wheeler, and H. Statz, *The Properties of the Thirty-Two Point Groups* (MIT Press, Cambridge, 1964).
[36] A. W. Joshi, *Elements of Group Theory for Physicists* (Wiley, New York, 1988).
[37] G. F. Quinteiro and J. Berakdar, Opt. Express **17**, 20465 (2009).
[38] D. Liang and X. P. Gao, Nano Lett. **12**, 3263 (2012).
[39] R. Winkler, Phys. Rev. B **62**, 4245 (2000).
[40] G. E. Murgida, D. A. Wisniacki, and P. I. Tamborenea, Phys. Rev. B **79**, 035326 (2009).
[41] M. Cygorek, P. I. Tamborenea, and V. M. Axt, Phys. Rev. B **93**, 205201 (2016).
[42] C. F. Fong, Y. Ota, S. Iwamoto, and Y. Arakawa, Opt. Express **26**, 21219 (2018).
[43] M. Cygorek, F. Ungar, P. I. Tamborenea, and V. M. Axt, Phys. Rev. B **95**, 045204 (2017).
[44] C. Thurn and V. M. Axt, Phys. Rev. B **85**, 165203 (2012).
[45] F. Ungar, M. Cygorek, P. I. Tamborenea, and V. M. Axt, Phys. Rev. B **91**, 195201 (2015).